

Analysis of Transitional Separation Bubbles on Infinite Swept Wings

R. L. Davis* and J. E. Carter†

United Technologies Research Center, East Hartford, Connecticut
and

E. Reshotko‡

Case Western Reserve University, Cleveland, Ohio

A previously developed two-dimensional local inviscid-viscous interaction technique for the analysis of airfoil transitional separation bubbles, ALESEP (airfoil leading-edge separation), has been extended for the calculation of transitional separation bubbles over infinite swept wings. A part of this effort, Roberts' empirical correlation, which is interpreted as a separated flow empirical extension of Mack's stability theory for attached flows, has been incorporated into the ALESEP procedure for the prediction of the transition location within the separation bubble. A series of two-dimensional calculations are presented as a verification of the prediction capability of the interaction technique with Roberts' transition model. Numerical tests have shown that this two-dimensional natural transition correlation may also be applied to transitional separation bubbles over infinite swept wings. Results of the interaction procedure are compared with Horton's detailed experimental data for separated flow over a swept plate, which demonstrates the accuracy of the present technique. The principal conclusion of this work is that the prediction of transitional separation bubbles over two-dimensional or infinite swept geometries is now possible using the present interacting boundary-layer approach.

Nomenclature

c = airfoil chord
 C_p = pressure coefficient
 C_f = skin-friction coefficient
 \tilde{f} = perturbation stream function
 F = velocity ratio, u/u_e
 G = total enthalpy ratio, H/H_e
 G_w = total enthalpy ratio at wall
 h = density ratio integral
 H = total enthalpy
 H_e = total enthalpy at edge of boundary layer
 l_t = arclength from separation to transition
 L = reference length
 m = perturbation mass flow
 n = coordinate normal to reference displacement surface
 N = coordinate measured normal to reference displacement surface from body surface
 Pr = Prandtl number
 Pr_T = turbulent Prandtl number
 Re_{l_t} = transition Reynolds number
 $Re_{\infty,c}$ = freestream Reynolds number based on airfoil chord
 $Re_{\infty,L}$ = freestream Reynolds number based on reference length
 s, S = coordinates along reference displacement surface
 Tu_{∞} = freestream turbulence level
 Tu_e = local turbulence level at edge of boundary layer
 u = velocity component normal to leading edge along x direction parallel to reference displacement surface
 u_e = local x component of boundary-layer edge velocity

u_e = local x component of boundary-layer edge velocity at separation
 v = velocity component along y direction normal to reference displacement surface
 V = transformed normal velocity in Prandtl transposition theorem
 V_{∞} = freestream velocity
 w = velocity component tangent to leading edge along z direction
 w_e = local z component of boundary-layer edge velocity
 W = velocity ratio, w/w_e
 x = coordinate direction normal to leading edge
 X = coordinate direction (absolute frame) parallel to freestream direction
 y = coordinate direction normal to surface
 z = coordinate direction tangent to leading edge
 Z = coordinate direction (absolute frame) perpendicular to freestream direction in reference plane of airfoil surface
 α = airfoil angle of attack, deg
 β = pressure gradient parameter
 δ = boundary-layer thickness
 δ^* = displacement thickness
 δ_{ref}^* = reference displacement surface thickness
 ϵ = eddy viscosity coefficient
 η = transformed normal coordinate
 Λ = sweep angle
 μ = molecular viscosity coefficient
 ν = kinematic viscosity coefficient
 ξ = transformed tangential coordinate
 ρ = density

Received Aug. 6, 1985; presented as Paper 85-1685 at the AIAA 18th Fluid Dynamics, Plasmadynamics and Lasers Conference, Cincinnati, OH, July 16-18, 1985; revision received Aug. 4, 1986. Copyright © American Institute of Aeronautics and Astronautics, Inc., 1985. All rights reserved.

*Research Engineer. Member AIAA.

†Manager, Computational Fluid Dynamics. Member AIAA.

‡Professor. Member AIAA.

Introduction

THERE has been renewed interest in recent years in the development of natural laminar flow (NLF) airfoils, which result in reduced drag from that incurred with turbulent flow airfoils. The performance of these laminar flow airfoils is critically dependent on the location of transition, which as pointed out in a recent study by Obara and Holmes,¹ often

occurs due to the separated shear layer of a closed transitional separation bubble. Although this separation bubble is generally of short streamwise extent, it is nonetheless a local site of strongly interacting viscous and inviscid flow, which cannot be analyzed by conventional boundary-layer analyses as was discussed by Obara and Holmes. Experimental studies²⁻⁷ have shown that for high Reynolds number flows, the viscous effects induced by a closed transitional separation bubble are contained within a relatively thin layer near the surface. This type of separated flow is well suited to analysis with interacting boundary-layer techniques that model the flowfield as separate inviscid and viscous regions coupled together through displacement thickness interaction. Significant developments in theoretical techniques,⁸⁻¹⁰ based on inviscid-viscous interaction theory, have been made for the calculation of two-dimensional transitional separation bubbles. For example, Vatsa and Carter¹⁰ developed the ALESEP (airfoil leading-edge separation) interaction analysis for the calculation of transitional separation bubbles on airfoils. This technique consists of a finite-difference boundary-layer scheme coupled to a Cauchy integral perturbation analysis for the inviscid flow using the semi-inverse coupling strategy. The focus of the current investigation has been the further development of this technique for the prediction of transitional separation bubbles. In particular, the ALESEP analysis has been extended to the flow over infinite swept wings, with some very encouraging comparisons presented with Horton's⁴ benchmark data to demonstrate this capability. This extension from two-dimensional airfoils to infinite swept wings represents an important first step in the eventual development of a fully three-dimensional analysis. In addition, the present approach has been significantly enhanced by the incorporation of Roberts'¹¹ empirical transition criteria for laminar separation bubbles. A brief discussion is presented that links Roberts' correlation for separated flow to Mack's¹² stability theory for attached flows. Computations are presented for two-dimensional airfoils and infinite swept wing flows that demonstrate the applicability of this correlation, provided the freestream turbulence level is known.

Inviscid-Viscous Interaction Analysis

In the present inviscid-viscous interaction analysis, the compressible three-dimensional boundary-layer equations for infinite swept wings are solved in inverse form iteratively with an incompressible Cauchy integral perturbation analysis for the inviscid flow. Iteration between the inviscid and viscous flow solutions is accommodated through the use of an update formula¹³ that modifies the specified displacement thickness distribution along the x direction, normal to the leading edge of the swept configuration, as shown in Fig. 1, based on the differences between the predicted inviscid and viscous velocities at the edge of the boundary layer in that direction. For infinite swept wings, the two-dimensional Cauchy integral analysis, described in Ref. 10, remains unchanged along a line perpendicular to the wing leading edge since the spanwise component of the boundary-layer edge velocity is constant and, therefore, is unaffected by the viscous displacement thickness. As shown by Moore¹⁴ for flows over infinite swept wings, the general three-dimensional displacement thickness reduces to the two-dimensional displacement definition that is based on the u -velocity component in the x direction.

Viscous Analysis

The viscous solution technique used for the investigation of swept transitional separation bubbles is an extension of the inverse procedure presented by Carter¹⁵ for two-dimensional flows. The nondimensional boundary-layer equations for an infinite swept body are written as follows in terms of the reference displacement surface coordinate system along a line perpendicular to the leading edge similar to that described in

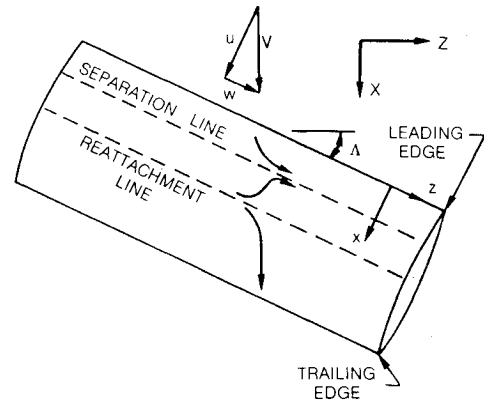


Fig. 1 Infinite swept wing coordinate system.

Ref. 10:

$$\frac{\partial \rho u}{\partial s} + \frac{\partial \rho v}{\partial n} = 0 \quad (1)$$

$$\rho u \frac{\partial u}{\partial s} + \rho v \frac{\partial u}{\partial n} = \rho_e u_e \frac{du_e}{ds} + \frac{\partial}{\partial n} \left[\mu \frac{\partial u}{\partial n} - \rho u'v' \right] \quad (2)$$

$$\rho u \frac{\partial w}{\partial s} + \rho v \frac{\partial w}{\partial n} = \frac{\partial}{\partial n} \left[\mu \frac{\partial w}{\partial n} - \rho w'v' \right] \quad (3)$$

$$\begin{aligned} \rho u \frac{\partial H}{\partial s} + \rho v \frac{\partial H}{\partial n} \\ = \frac{\partial}{\partial n} \left[\frac{\mu}{Pr} \frac{\partial H}{\partial n} - \rho v'H' + \frac{\mu}{2} \left(1 - \frac{1}{Pr} \right) \frac{\partial (u^2 + w^2)}{\partial n} \right] \end{aligned} \quad (4)$$

The v component of velocity and the n coordinate are scaled by $\sqrt{Re_{\infty, L}}$. The boundary conditions imposed on the governing equations at $n = -\delta_{ref}^*$ and as $n \rightarrow \infty$ are, respectively,

$$u = v = w = 0$$

$$H \text{ or } \frac{\partial H}{\partial n} \text{ specified} \quad (5a)$$

$$u \rightarrow u_e$$

$$w \rightarrow w_e = \sin \Lambda$$

$$H \rightarrow H_e \quad (5b)$$

Equations (1-4) are transformed into the ξ, η coordinate system through the use of the Levy-Lees type of variables described in Ref. 10. In order to simplify the boundary conditions, the velocity components and stagnation enthalpy are normalized by their corresponding edge values:

$$F = \frac{u}{u_e}, \quad W = \frac{w}{w_e}, \quad G = \frac{H}{H_e} \quad (6)$$

The normal component of velocity is replaced by the introduction of a perturbation stream function \tilde{f} , also described in Ref. 10. Use of this perturbation stream function is the key step in this formulation for the imposition of the prescribed displacement thickness. With the continuity equation replaced with the stream function equation and after use of the Prandtl transposition theorem as discussed in Ref. 10, the governing equations are written in transformed coordinates as

$$\frac{\partial \tilde{f}}{\partial \eta} = \frac{m}{\sqrt{2\xi}} (1 - \eta - h) \frac{\partial F}{\partial \eta} \quad (7)$$

$$\begin{aligned}
m^2 F \frac{\partial F}{\partial \xi} - m \frac{\partial}{\partial \xi} [\sqrt{2\xi} \tilde{f} + mF(\eta - 1 + h)] \frac{\partial F}{\partial \eta} \\
= m^2 \beta \left\{ G - F^2 \left(1 + \frac{w_e^2/u_e^2}{1 + [(\gamma - 1)/2] M_e^2} \right) \right. \\
\left. - W^2 \left(\frac{[(\gamma - 1)/2] M_e^2 w_e^2/u_e^2}{1 + [(\gamma - 1)/2] M_e^2} \right) \right\} + \frac{\partial}{\partial \eta} \left[\left(1 + \frac{\epsilon}{\mu} \right) \ell \frac{\partial F}{\partial \eta} \right]
\end{aligned} \quad (8)$$

$$\begin{aligned}
m^2 F \frac{\partial W}{\partial \xi} - m \frac{\partial}{\partial \xi} [\sqrt{2\xi} \tilde{f} + mF(\eta - 1 + h)] \frac{\partial W}{\partial \eta} \\
= \frac{\partial}{\partial \eta} \left[\left(1 + \frac{\epsilon}{\mu} \right) \ell \frac{\partial W}{\partial \eta} \right]
\end{aligned} \quad (9)$$

$$\begin{aligned}
m^2 F \frac{\partial G}{\partial \xi} - m \frac{\partial}{\partial \xi} [\sqrt{2\xi} \tilde{f} + mF(\eta - 1 + h)] \frac{\partial G}{\partial \eta} \\
= \frac{1}{Pr} \frac{\partial}{\partial \eta} \left[\ell \left(1 + \frac{\epsilon}{\mu} \frac{Pr}{Pr_T} \right) \frac{\partial G}{\partial \eta} \right] \\
+ \frac{[1 - (1/Pr)](\gamma - 1) M_e^2}{\{1 + [(\gamma - 1)/2] M_e^2\} (u_e^2 + w_e^2)} \\
\times \frac{\partial}{\partial \eta} \left[\ell \left(u_e^2 F \frac{\partial F}{\partial \eta} + w_e^2 W \frac{\partial W}{\partial \eta} \right) \right]
\end{aligned} \quad (10)$$

where

$$\begin{aligned}
\beta = \frac{1}{M_e} \frac{dM_e}{d\xi}, \quad \ell = \frac{\rho \mu}{\rho_e \mu_e}, \\
h = \int_0^\infty \left(\frac{\rho_e}{\rho} - 1 \right) d\eta, \quad m = \rho_e u_e \delta^*
\end{aligned} \quad (11)$$

In these equations, the Reynolds stresses have been related in the usual manner to the mean velocity and temperature gradients through the use of an eddy viscosity coefficient. The turbulence model used in this investigation will be discussed in the next section. Equations (7–10) are solved for F , W , G , \tilde{f} , and β for a prescribed streamwise distribution of m , subject to the following boundary conditions at $\eta = 0$ and as $\eta \rightarrow \infty$, respectively:

$$\begin{aligned}
F = W = \tilde{f} = 0 \\
G = G_w \text{ or } \frac{\partial G}{\partial \eta} \Big|_w \text{ specified}
\end{aligned} \quad (12a)$$

$$\begin{aligned}
F = W = G \rightarrow 1 \\
\tilde{f} \rightarrow 0
\end{aligned} \quad (12b)$$

These equations can also be solved in the direct mode with β prescribed and the outer boundary condition $\tilde{f} = 0$ eliminated. The numerical solution of these equations for the direct and inverse modes is obtained through the use of an implicit finite-difference technique similar to that used by Carter,¹⁵ which is first-order accurate in the ξ direction and second-order accurate in the η direction.

A windward differencing scheme similar to that described in Ref. 16 is used in the reversed flow regions for the streamwise convection terms in Eqs. (8–10). This windward differencing scheme has been found to have an insignificant effect on the predicted results as compared to similar calculations using the FLARE (Reyhner and Flugge-Lotz¹⁷) approximation with the only exception being the spanwise (z direction) velocity profiles.

Turbulence Model

In the previous two-dimensional interaction calculations presented in Refs. 10 and 16, the Cebeci-Smith¹⁸ turbulence model was used to determine the eddy viscosity coefficient ϵ . With the extension of the interaction approach to include flow over infinite swept wings, a three-dimensional version of this model¹⁹ has been used to calculate the eddy viscosity coefficients in the x and z directions. In the current investigation, the turbulence field has been assumed to be isotropic.

In contrast to previous two-dimensional work on transitional separation bubbles,^{10,16} it was found necessary in the present calculations for the Horton swept plate experiment to modify the Clauser constant in the outer layer of the turbulence model in order to obtain flow reattachment. Without this increase in the Clauser constant, reattachment of the flow downstream of transition did not occur, leading to stalled flow and subsequent divergence of the numerical calculation. Since the Cebeci-Smith model was originally developed for attached flows, it is expected that some changes in this model are needed for the analysis of separated flows. Kim et al.²⁰ deduced from experimental data for the reattaching flow downstream of a backward-facing step that the Clauser constant increases from the value of 0.0168 in attached flows to levels as great as 0.085 both upstream and downstream of reattachment. In the present computations corresponding to Horton's⁴ swept plate experiment, a Clauser constant of 0.084 was found to produce the best agreement with the experimental pressure distribution and velocity profiles. This value of the Clauser constant was held fixed in the entire turbulent portion of the flowfield. A similar modification to the Clauser constant was described by Cebeci et al.²¹ for some recent interaction analyses of turbulent separated flow.

Transition Prediction

The computation of airfoil transitional separation bubbles requires the use of some transitional criterion that establishes the length of the laminar separated shear layer as a function of the turbulence level of the external flow. The variation of transition Reynolds number with freestream turbulence level has been estimated by Mack¹² for the Falkner-Skan family of laminar boundary layers. Using typical wind-tunnel turbulence spectra as input to a growth calculation based on linear stability theory, Mack found that transition due to freestream turbulence for a flat plate boundary layer could be correlated with an amplitude ratio from linear stability theory of e^n , where

$$n = -8.43 - 2.4 \mathcal{C}_n (Tu_\infty) \quad (13)$$

Using this transition criterion, Mack obtained results for the Falkner-Skan family that are shown in Fig. 2. The experimental data shown in Fig. 2 are those taken by Dryden²² for flow over a flat plate. The curves are remarkably similar in shape but show significant decrease in transition Reynolds number as the pressure gradient β becomes more adverse.

The laminar portion of a separation bubble is not represented within the traditional Falkner-Skan flows. Rather, it is better represented by the family of reversed flow solutions to the Falkner-Skan-Hartree equation that were calculated by Stewartson²³ and by Christian and Hankey.²⁴ The stability characteristics of these reversed flow profiles were calculated recently by Gleyzes, Cousteix, and Bonnet.⁸ In principle then, the curves presented by Mack could be extended to cover the Stewartson profiles using the results of Ref. 8.

The pressure gradient history of a laminar separation bubble from the point of separation to the transition point is not representable as any single similarity profile of the Stewartson family. It is felt, however, that it is a reproducible composite of them. Thus, it can be expected that the transition Reynolds numbers as a function of external turbulence level should be represented by a curve resembling those presented by Mack

for the Falkner-Skan family but at a lower level than those for the attached flows. For the present use, this curve will be obtained from experimental results reported in the literature.

Roberts^{11,25} put together such a correlation in terms of a turbulence factor based on both turbulence level and scale rather than on turbulence level alone. This representation is very appropriate as it is an approximate way of representing the effects of disturbance spectrum on transition. In any given facility, however, there is usually a one-to-one relation between turbulence level and turbulence factor. Wind tunnels of comparable design would have comparable relationships between turbulence level and turbulence factor. Since the scale of turbulence is not uniformly available for all the experiments considered in developing and applying the correlation, the correlation will be presented in terms of turbulence level alone.

For the calculations presented herein, the transition length has been estimated according to the following form of Roberts' relation:

$$Re_{1_t} = \frac{u_e l_t}{\nu} = 25,000 \log_{10} [\coth(17.32 Tu_e)] \quad (14)$$

This relation is shown in Fig. 3, together with the data points from the investigations on which it is based.^{2-5,26-28} Because of uncertainties in evaluating some of the points, and because of some scatter in the plot, the above relation must be regarded as provisional, pending further detailed study of the data included in Fig. 3, as well as any other relevant data that may become available. More particularly, transition in many low-turbulence wind tunnels is limited by acoustic disturbances rather than by freestream turbulence, so a correlation based on turbulence alone may overestimate the length to transition. Similar considerations apply to flight application of this approach.

Further, it is felt that the above criterion may also be applied to the separation bubble on a swept wing. This is justified by the following argument. Transition in three-dimensional boundary layers tends to be determined by the component profile that displays the largest growth rate. On a swept wing where the spanwise profile is an attached profile, it is expected that the chordwise separated, reversed flow is less stable than even the cross flow, and so it is recommended that the above criterion be used in estimating the chordwise length to transition.

In the implementation of the Roberts transition correlation into the present viscous analysis, the transition location was allowed to change only during the first 20 global interaction iterations. After the twentieth iteration, the transition location was frozen for the remainder of the interaction calculation. It was found from numerical tests that without freezing the transition location at some point during the iterative process, convergence could not be obtained since a limit cycle occurred due to oscillations in the predicted transition location. This approximate treatment should have only a minor impact since the changes in the edge velocity after 20 interaction iterations were small.

Results and Discussion

With the implementation of the Roberts natural transition correlation into the ALESEP inviscid-viscous interaction procedure, a series of two-dimensional cases were calculated and compared to previously published results in Refs. 10 and 16, where transition was prescribed near the "break point" in the experimental pressure distribution. Calculations corresponding to the Gaster³ Series I, No. IV experiment and the Gault² modified NACA-0010 airfoil and NACA 663-018 airfoil experiments were made to evaluate the accuracy of the natural transition model. Upon verification of the Roberts correlation, the extended ALESEP interaction procedure for infinite swept wings was tested against the experimental data of Horton for the separated flow over a swept flat plate. The Roberts corre-

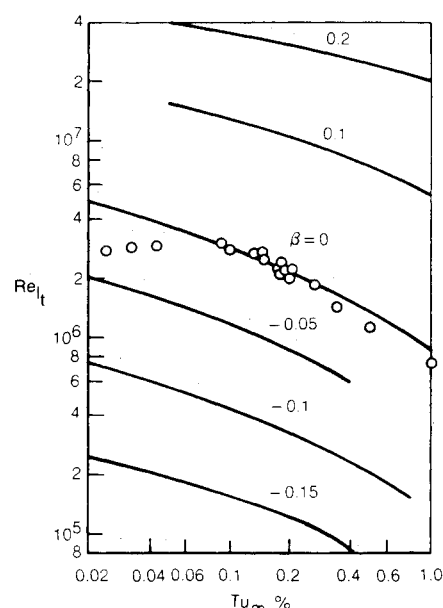


Fig. 2 Effect of freestream turbulence on the transition Reynolds number of Falkner-Skan boundary layers.¹²

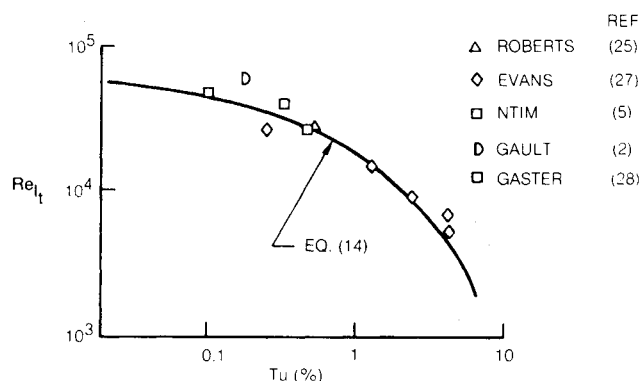


Fig. 3 Roberts-type correlation of experimental data.

lation was also used in this calculation to determine the transition location. Windward differencing of the convection terms in the boundary-layer equations has been used for all the calculations presented herein except where noted. As stated before, similar calculations have been performed with the FLARE approximation and have given essentially identical results in terms of the surface pressure and skin-friction distributions.

Natural Transition Model Computations

Gaster Experiment

The experiment performed by Gaster³ consisted of a separation bubble on a flat plate induced by the pressure field generated by the placement of an inverted airfoil near the plate. Vatsa and Carter¹⁰ originally calculated the flowfield corresponding to this experiment using the ALESEP analysis with a prescribed transition model. They found that the best match between the numerical results and the experimental data was obtained when instantaneous transition was prescribed at $s/L = 1.0125$. The ALESEP analysis has now been used to predict the flowfield for this experiment using the same computational grid and reference conditions used by Vatsa and Carter but with instantaneous transition predicted using the Roberts model. The freestream turbulence level for this experiment as used in Eq. (14) for the Roberts correlation is 0.0025. Figure 4 shows a comparison of the predicted numerical results and the experimental data for this calculation.

tion. Excellent agreement is obtained between the present prediction and the data for this case, as should be expected, since the Gaster experimental data were part of the data base used by Roberts to formulate his model. With the use of the Roberts transition model, transition was predicted to occur at $s/L = 1.025$. This location is quite close to the assumed position of transition and therefore explains the good agreement obtained between the two theoretical results in Fig. 4.

Gault NACA-0010 Airfoil

The NACA-0010 modified airfoil tested experimentally by Gault² at an 8-deg angle of attack and a chord Reynolds number of 2.0×10^6 was calculated originally by Vatsa and Carter¹⁰ and later in Ref. 16. In both instances, transition was initiated at $s/c = 0.0283$, with a transition length of 0.0161. The Dhawan and Narasimha²⁹ intermittency distribution was used to vary the flow smoothly from laminar to turbulent motion over the transition length. The intermittency factor reached a value of 0.5 at a location of $s/c = 0.0350$. The predicted separation and reattachment locations for these calculations were $s/c = 0.0156$ and $s/c = 0.0439$, respectively. This case has been repeated using the Roberts instantaneous natural transition model with the same computational grid and reference conditions. The freestream turbulence level in this experiment was 0.002. Figure 5 shows the comparison between the present and previous interaction results and the experimental data. Transition was predicted to occur at $s/c = 0.0375$ with the Roberts model, which is somewhat downstream of that used earlier in the forced transition model. Although this difference corresponds to only about a 0.25% change in transition location in terms of the airfoil chord, it has a rather pronounced effect on the local pressure distribution in comparison to the experimental data. This result is not surprising, because it was demonstrated in Refs. 30 and 31 that the detailed flow properties near the transitional separation bubble are extremely sensitive to the transition location. In this case, a slight delay in transition has resulted in a larger separation bubble than that found previously and, hence, a reduction in the peak suction pressure level. Nonetheless, it is encouraging that this natural transition model can be used in conjunction with the present interacting boundary-layer theory to provide an approximate prediction of the complex flowfield near a transitional separation bubble.

Gault NACA 66₃-018 Airfoil

A final two-dimensional case that has been analyzed is the NACA 66₃-018 midchord separation bubble tested experimentally by Gault² at a chord Reynolds number of 2.0×10^6 . The freestream turbulence was 0.002 for this experiment. This case was originally calculated in Ref. 16 using the ALESEP analysis with the McDonald-Fish-Kreskovsky^{32,33} turbulence

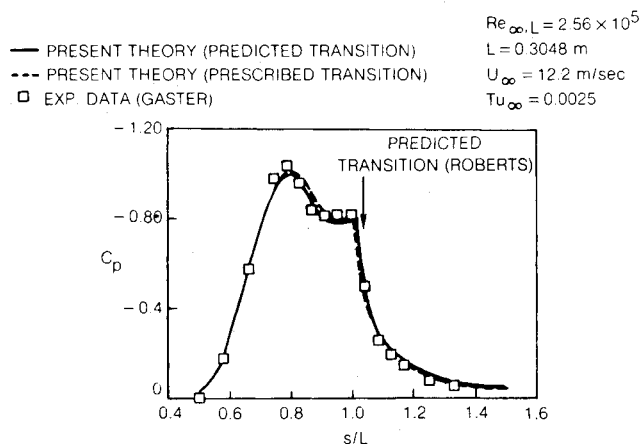


Fig. 4 Comparison of predicted pressure distribution with Gaster experimental data.

model. This case has been recalculated in the present study using the Cebeci-Smith turbulence model,¹⁸ using the same computational grid and reference conditions as reported in Ref. 16. In this case, the best match between the numerical results and the experimental data was obtained when transition was specified to occur instantaneously at $x/c = 0.725$. Figure 6 shows the predicted pressure distributions obtained with the Roberts model and the forced transition model in comparison with the experimental data of Gault. In contrast to the NACA-0010 case, Roberts' criterion predicts transition ahead of the "break" in the pressure distribution and, hence, a smaller separation bubble is deduced than that with the forced model. Specifically, transition was predicted at $x/c = 0.690$, which corresponds to a change in the transition location from the prescribed location of 4% in terms of the airfoil chord. However, in terms of the predicted separation bubble length of the prescribed transition calculation in which separation is at $x/c = 0.647$ and reattachment at $x/c = 0.734$, this difference corresponds to about a 40% change. Roberts¹¹ found similar results for this case using his global interaction model.

The results of these two-dimensional separation bubble calculations have shown that in terms of a global airfoil prediction scheme, the Roberts correlation may be a good method to predict the approximate location of transition when a closed separation bubble is formed. However, if details of the flowfield in the immediate vicinity of the separation bubble are required, modifications to this correlation are needed to improve the accuracy and generality.

Infinite Swept Wing

Horton Experiment

The extended ALESEP inviscid-viscous interaction procedure for infinite swept wings has been assessed with the experimental data of Horton.⁴ In Horton's experiment, a swept circular cylinder was placed above a 26.5-deg swept flat plate to induce a favorable pressure gradient followed by an adverse pressure gradient similar to that at the leading edge of a wing. Horton carefully controlled the experimental parameters to establish a closed transitional separation bubble on the flat plate in the adverse pressure gradient region of the flow. The spanwise repeatability of measured pressure distributions showed that despite the presence of separation, the experiment satisfied the infinite swept wing conditions. The particular case chosen from this experiment for the present comparison was that for a freestream velocity of 15.82 m/s (51.9 ft/s). The Reynolds number of the flow was 2.77×10^4 based on a reference length of 0.0254 m (1 in.), and the freestream

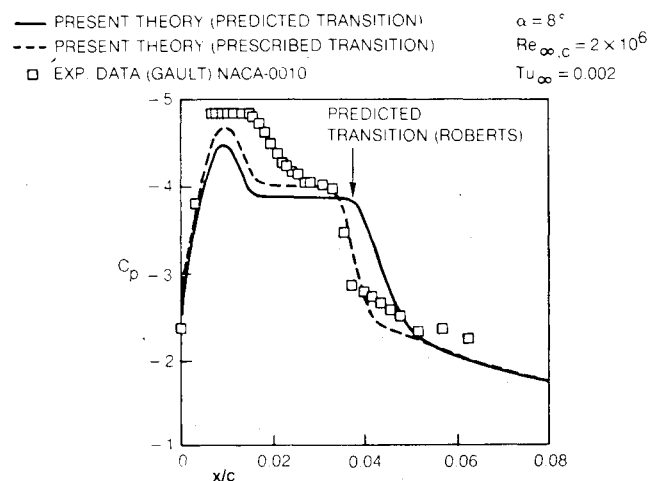


Fig. 5 Comparison of predicted pressure distribution with Gault experimental data for NACA-0010 (modified) airfoil.

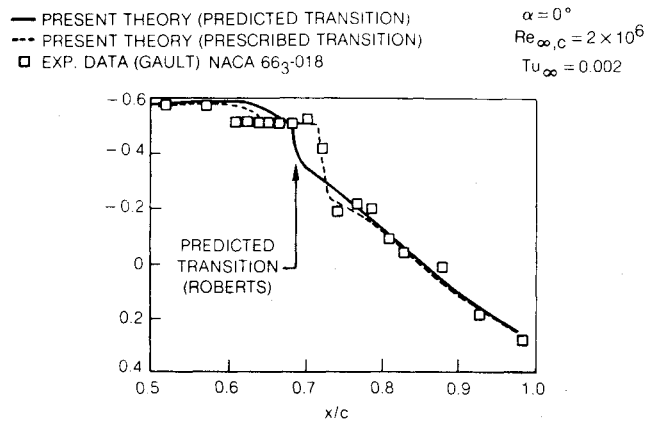


Fig. 6 Comparison of predicted pressure distribution with Gault experimental data for NACA 663-018 airfoil.

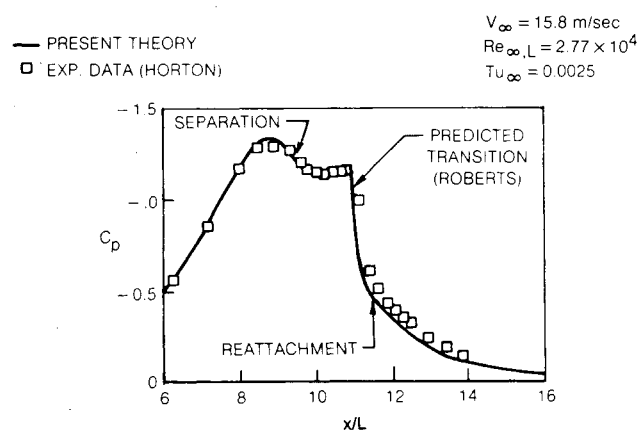


Fig. 7 Comparison of predicted pressure distribution with Horton swept plate experimental data.

turbulence level was 0.0025. The inviscid solution calculated by Woodward³⁴ for Horton's configuration was used as the inviscid reference solution. The corresponding reference displacement thickness distribution that also appears explicitly in the Cauchy integral analysis¹⁰ was obtained from a direct (attached flow) fully turbulent boundary-layer calculation in which the inviscid reference solution was used for the prescribed boundary-layer edge velocity component. The upstream velocity profile for the interaction calculation was obtained from a direct laminar boundary-layer calculation from the leading edge of the swept plate to a downstream position, $x/L = 7.0$, which is upstream of the strong interaction region. The interaction calculation was computed with 91 computational points spaced uniformly in the x direction, normal to the leading edge, between $x/L = 7.0$ and $x/L = 16.0$, and 100 points in the vertical direction with the minimum spacing placed at the wall. An underrelaxation parameter of 0.5 associated with the update formula of the interaction scheme was used in both the windward and FLARE calculations, which were performed for this case.

Figures 7 and 8 show good agreement between the predicted results and the experimental data for the pressure coefficient and displacement thickness distributions, respectively. These results are in part due to the excellent agreement between the transition location predicted by the Roberts correlation and the observed experimental transition location. The predicted separation, transition, and reattachment locations are indicated with arrows in Figs. 7 and 8. Separation was predicted to occur at $x/L = 9.55$. Transition from laminar to turbulent flow was predicted by the Roberts correlation to occur at $x/L = 11.1$. The onset of transition causes a sudden

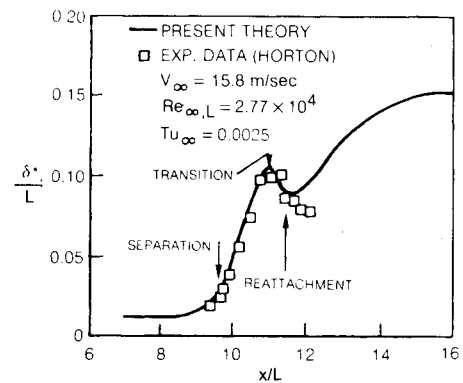


Fig. 8 Comparison of predicted displacement thickness distribution with Horton swept plate experimental data.

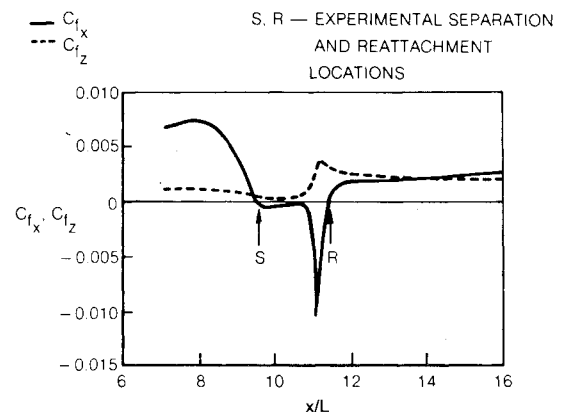


Fig. 9 Predicted skin-friction components for Horton swept plate experimental data.

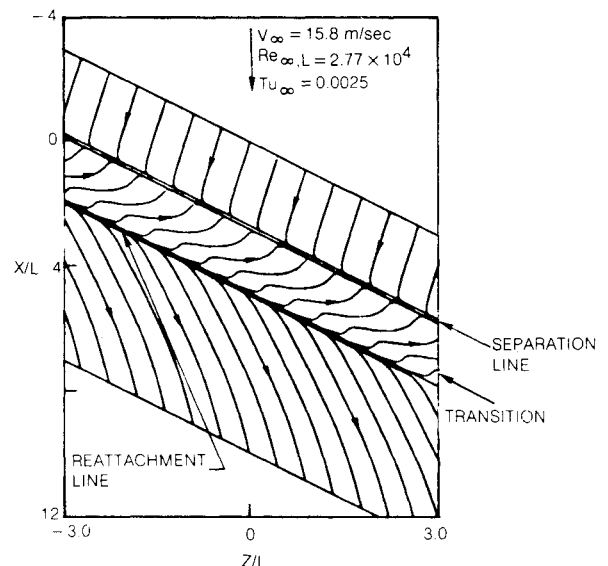


Fig. 10 Predicted limiting streamlines corresponding to Horton swept plate experiment.

increase in the pressure coefficient and a corresponding decrease in the displacement thickness, with subsequent reattachment occurring a short distance downstream at $x/L = 11.43$. The onset of transition also corresponds to the sharp rise in the x component of skin friction shown in Fig. 9. Excellent agreement is observed in Fig. 9 between the predicted and experimental separation and reattachment locations.

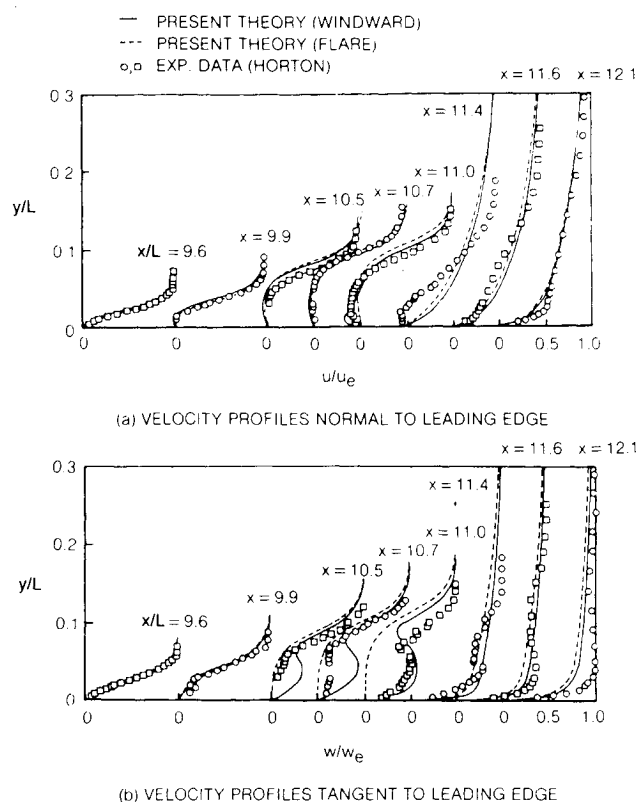


Fig. 11 Comparison of predicted results with Horton swept plate experimental data.

For infinite swept wings, separation and reattachment correspond to lines parallel to the leading edge where $C_{fz} = 0$. The z component of skin friction, also shown in Fig. 9, remains positive through the separated flow region. This outward spanwise migration of flow in the separation bubble is graphically shown in the predicted limiting streamline pattern of Fig. 10. In this figure, the limiting streamlines are plotted in the absolute X, Z coordinate system shown in Fig. 1. The X direction in this figure has been translated such that the start of the interaction calculation, which is located at $x/L = 7.0$ ($X/L = 7.82$) was at 0.0. The streamline pattern shown in Fig. 10 supports the trapped vortex pattern that Horton deduced from his experimental data. In this trapped vortex, the flow inside the separation bubble consists of a swirling helical motion in the positive spanwise direction brought about by the superposition of the closed chordwise separation bubble with the outward flow in the spanwise direction.

Figure 11 shows a comparison of the predicted u/u_e and w/w_e velocity profiles corresponding to the x and z directions, respectively, with the experimental data at eight different locations normal to the leading edge. The predicted velocity profiles for the calculation in which the FLARE approximation was used are also shown in this figure for comparison. The u/u_e velocity profiles obtained with the windward and FLARE schemes, as shown in Fig. 11a, are in close agreement with each other, as well as with the experimental data. The largest differences between the predictions and the experimental data are in the region just downstream of where transition occurs ($x/L = 11.1$). The predicted w/w_e velocity profiles shown in Fig. 11b also show reasonably good agreement with the experimental data, except in the region near transition. However, in contrast with the u/u_e profiles, the windward and FLARE results differ substantially in the separation bubble region. These differences indicate that windward differencing is important in quasi-three-dimensional flow and, hence, should be important in three-dimensional calculations.

Concluding Remarks

In this paper, the development of an inviscid-viscous interaction analysis for the prediction of airfoil transitional separation bubbles has been continued with the incorporation of the Roberts correlation for the prediction of the transition location within the bubble and the extension of the analysis to flows over infinite swept wings. Results from several two-dimensional cases indicate that the Roberts transition calculation is an accurate method for the prediction of the transition location within the separation bubble if detailed results in the vicinity of the separation bubble are not required. Modifications to this correlation should be made from carefully conducted experiments, however, to make it more accurate and general. Results have been shown which demonstrate that interacting boundary-layer theory is capable of predicting transitional separation bubbles over infinite swept wings. These results provide valuable insight, which will guide the future development of procedures for the fully three-dimensional flowfield that exists in swept separation bubbles.

Acknowledgments

The work reported in this paper was supported in part by the NASA Langley Research Center under Contract NAS1-16585. The ALESEP computer program and documentation are available on request to NASA or the authors. The authors express their gratitude to the technical monitor, Mr. Joel L. Everhart, for his assistance during the execution of this work. The authors wish to thank Dr. Harry P. Horton for providing additional information and technical discussions concerning his infinite swept plate experiment. Also, the authors express their gratitude to Mr. David Edwards for his help in implementing the Roberts transition correlation into the interaction procedure.

References

- 1 Obara, C.J. and Holmes, B.J., "Flight-Measured Laminar Boundary-Layer Transition Phenomena Including Stability Theory Analysis," NASA TP-2417, April 1985.
- 2 Gault, D.E., "An Experimental Investigation of Separated Laminar Flow," NASA TN-3505, Sept. 1955.
- 3 Gaster, M., "The Structure and Behavior of Laminar Separation Bubbles," AGARD CP-4, 1966, pp. 819-854.
- 4 Horton, H.P., "Laminar Separation Bubbles in Two and Three Dimensional Incompressible Flow," Ph.D. Thesis, University of London, 1968.
- 5 Ntim, B.A., "A Theoretical and Experimental Investigation of Separation Bubbles," Ph.D. Thesis, University of London, 1969.
- 6 Mueller, T.J. and Batill, S.M., "Experimental Studies of the Laminar Separation Bubbles on a Two-Dimensional Airfoil at Low Reynolds Numbers," AIAA Paper 80-1440, 1980.
- 7 Bursnall, W.J. and Loftin, L.K. Jr., "Experimental Investigation of Localized Regions of Laminar-Boundary-Layer Separation," NACA TN-2338, April 1951.
- 8 Gleyzes, C., Cousteix, J., and Bonnet, J.L., "A Calculation Method of Leading Edge Separation Bubbles," *Proceedings of Second Symposium on Numerical and Physical Aspects of Aerodynamic Flows*, California State Univ., Long Beach, CA, Jan. 1983.
- 9 Kwon, O.K. and Pletcher, R.H., "Prediction of Incompressible Separated Boundary Layer Including Viscous-Inviscid Interaction," *Journal of Fluids Engineering*, Vol. 101, Dec. 1979, pp. 466-472.
- 10 Vatsa, V.N. and Carter, J.E., "Analysis of Airfoil Leading-Edge Separation Bubbles," *AIAA Journal*, Vol. 22, Dec. 1984, pp. 1697-1704.
- 11 Roberts, W.B., "Calculation of Laminar Separation Bubbles and Their Effect on Airfoil Performance," *AIAA Journal*, Vol. 18, Jan. 1980, pp. 25-30.
- 12 Mack, L.M., "Transition Prediction and Linear Stability Theory," AGARD CP-224, 1977, pp. 1-1-1-22.
- 13 Carter, J.E., "A New Boundary Layer Inviscid Iteration Technique for Separated Flow," AIAA Paper 79-1450, July 1979.
- 14 Moore, F.K., "Displacement Effect of a Three-Dimensional Boundary Layer," NACA Rept. 1124, 1953.
- 15 Carter, J.E., "Inverse Boundary-Layer Theory and Comparison With Experiment," NASA TP-1208, Sept. 1978.

¹⁶Davis, R.L. and Carter, J.E., "Analysis of Airfoil Transitional Separation Bubbles," AIAA Paper 84-1613, 1984.

¹⁷Reyhner, T.A. and Flugge-Lotz, I., "The Interaction of a Shock Wave with a Laminar Boundary Layer," *International Journal of Non-Linear Mechanics*, Vol. 3, No. 2, June 1968, pp. 173-179.

¹⁸Cebeci, T. and Smith, A.M.O., *Analysis of Turbulent Boundary Layers*, Academic Press, Orlando, FL, 1974.

¹⁹Cebeci, T., Kaups, K., Mosinskis, G.J., and Rehn, J.A., "Some Problems of the Calculation of Three-Dimensional Boundary Layer Flows on General Configurations," NASA CR-2285, July 1973.

²⁰Kim, J., Kline, S.J., and Johnston, J.P., "Investigation of a Reattaching Turbulent Shear Layer: Flow Over a Backward-Facing Step," *Transactions of the ASME*, Vol. 102, Sept. 1980, pp. 302-308.

²¹Cebeci, T., Clark, R.W., Chang, K.C., Halsey, N.D., and Lee, K., "Airfoils with Separation and the Resulting Wakes," *Proceedings of Third Symposium on Numerical and Physical Aspects of Aerodynamic Flows*, California State Univ., Long Beach, CA, Jan. 1985.

²²Dryden, H.L., "Transition from Laminar to Turbulent Flow," *Turbulent Flows and Heat Transfer*, edited by C.C. Lin, Princeton Univ., Princeton, NJ, 1959, pp. 1-74.

²³Stewartson, K., "Further Solutions of the Falkner-Skan Equation," *Proceedings of the Cambridge Philosophical Society*, Vol. 50, 1954, pp. 454-465.

²⁴Christian, J.W. and Hankey, W.L., "Similar Solutions of the Attached and Separated Compressible Boundary Layer with Heat Transfer and Pressure Gradient," ARL 70-0023, 1970.

²⁵Roberts, W.B., "A Study of the Effect of Reynolds Number and Laminar Separation Bubbles on the Flow Through Axial Compressor

Cascades," D.Sc. Thesis, Université Libre de Bruxelles and VKI, May 1973.

²⁶Horton, H.P., "A Semi-Empirical Theory for the Growth and Bursting of Laminar Separation Bubbles," Aeronautical Research Council, England, Current Paper 1073, 1969.

²⁷Evans, B.J., "Effects of the Free Stream Turbulence on Blade Performance in a Compressor Cascade," Cambridge Univ., Engineering Dept. Rept. Turbo/TR25, 1971.

²⁸Gaster, M., "The Structure and Behavior of Laminar Separation Bubbles," NPL Aero. Rept. 1181, ARC 28.226, 1966.

²⁹Dhawan, S. and Narasimha, R., "Some Properties of Boundary Layer Flow During Transition from Laminar to Turbulent Motion," *Journal of Fluid Mechanics*, Vol. 3, 1958.

³⁰Carter, J.E. and Vatsa, V.N., "Analysis of Airfoil Leading Edge Separation Bubbles," NASA CR-165935, May 1982.

³¹Davis, R.L. and Carter, J.E., "Analysis of Airfoil Transitional Separation Bubbles," NASA CR-3791, 1984.

³²McDonald, H. and Fish, R.W., Practical Calculation of Transitional Boundary Layers, *International Journal Heat Mass Transfer*, Vol. 16, Sept. 1973, pp. 1729-1944.

³³McDonald, H. and Kreskovsky, J.P., "Effect of Free Stream Turbulence on the Turbulent Boundary Layer," *International Journal of Heat and Mass Transfer*, Vol. 17, July 1974, pp. 705-716.

³⁴Woodward, D.S., "An Investigation of the Parameters Controlling the Behaviour of Laminar Separation Bubbles," RAE TM Aero 1003, Aug. 1967.

From the AIAA Progress in Astronautics and Aeronautics Series...

COMBUSTION DIAGNOSTICS BY NONINTRUSIVE METHODS - v. 92

*Edited by T.D. McCay, NASA Marshall Space Flight Center
and
J.A. Roux, The University of Mississippi*

This recent Progress Series volume, treating combustion diagnostics by nonintrusive spectroscopic methods, focuses on current research and techniques finding broad acceptance as standard tools within the combustion and thermophysics research communities. This book gives a solid exposition of the state-of-the-art of two basic techniques—coherent antistokes Raman scattering (CARS) and laser-induced fluorescence (LIF)—and illustrates diagnostic capabilities in two application areas, particle and combustion diagnostics—the goals being to correctly diagnose gas and particle properties in the flowfields of interest. The need to develop nonintrusive techniques is apparent for all flow regimes, but it becomes of particular concern for the subsonic combustion flows so often of interest in thermophysics research. The volume contains scientific descriptions of the methods for making such measurements, primarily of gas temperature and pressure and particle size.

Published in 1984, 347 pp., 6×9, illus., \$49.50 Mem., \$69.50 List; ISBN 0-915928-86-8

TO ORDER WRITE: Publications Order Dept., AIAA, 1633 Broadway, New York, N.Y. 10019